U.S. Geological Survey Final Technical Report

Award No. 03HQGR0021

Recipient: University of California at Santa Barbara

Kinematic Mapping of 3D Fault Planes in Southern California

Principal Investigator: Craig Nicholson

Collaborators: Marc J. Kamerling and Christopher C. Sorlien

Institute for Crustal Studies and Marine Science Institute,
University of California
1140 Girvetz Hall, Santa Barbara, CA 93106

NEHRP Program Elements: SC-I & SC-II

Research supported by the U.S. Geological Survey (USGS), Department of the Interior, under USGS Award No. **03HQGR0021**. The views and conclusions contained in this document are those of the authors, and should not be interpreted as necessarily representing the official policies, either expressed or implied, of the U.S. Government.

Kinematic Mapping of 3D Fault Planes in Southern California

Craig Nicholson

Abstract

Accurate assessment of the seismic hazard in southern California requires an accurate and complete description of the active faults in three dimensions. Dynamic rupture behavior, fault segmentation, and the interaction between faults all depend on the location, orientation, geometry, and sense of slip of these 3D fault surfaces. Several groups have now produced improved catalogs of the relocated earthquake activity in southern California. These catalogs comprise over 300,000 earthquake hypocenters since 1988, and over 200,000 well-determined earthquake focal mechanisms. Although many of these earthquakes do occur along mapped surface traces of major faults, many still do not. These extensive catalogs need to carefully examined and analyzed, not only for the accuracy and resolution of the earthquake hypocenters, but also for kinematic consistency of the spatial pattern of fault slip and the orientation of 3D fault surfaces at seismogenic depths.

The San Andreas fault system in southern California has a high probability of generating a major damaging earthquake. How big, when and where such an event will be generated appears to largely depend on subtle, second-order variations in stress, strength and fault geometry, such as fault bends, offsets, changes in fault dip, or other fault discontinuities that control fault segmentation and rupture behavior. Rupture along major through-going faults in southern California thus appears to be strongly affected by local fault geometry and velocity structure, as well as the sense of slip and relative orientation of secondary structures, such as left-lateral conjugate cross faults, tear faults, and low-angle basal detachments. Identification of these features, especially at seismogenic depths, often depends on careful kinematic analysis of the earthquake hypocenters and focal mechanisms in both space and time.

For this project, owing to limitations in funding, the seismicity patterns in and around the Santa Barbara-Ventura area were investigated to help identify and map active subsurface fault surfaces in 3D, and to improve our understanding of the regional tectonic framework controlling contemporary crustal deformation in southern California. This area includes various strands of the North Channel, Pitas Point, Red Mountain, Arroyo Parida, and Santa Ynez faults. Detailed kinematic analysis of accurate relocated earthquake hypocenters and focal mechanisms were used to resolve 3D fault planes and patterns of strain accommodation. Where available, other sets of geologic and geophysical data, including topography, gravity, geologic mapping, seismic reflection and subsurface well data were also used. The results suggest that several of these major fault strands, both onshore and offshore of southern California, merge at depth to form a single active North Channel–Pitas Point–Red Mountain fault system. In addition, the 3D geometry and slip on these active subsurface faults often exhibit strain partitioning on both high- and low-angle structures as contemporary plate motion is accommodated on combinations of reactivated, inherited tectonic features, and newer faults that form as the fault system evolves with time.

Introduction

Accurate assessment of the seismic hazard in southern California requires accurate and complete 3D fault maps. Many aspects of seismic hazard are controlled by the location, geometry, and style of active faults. In southern California, these structures include both relatively high-angle strike-slip and oblique-slip faults—many of which intersect and are mapped at the surface, as well as low-to-moderate-angle faults, some of which are blind and are difficult to identify. The 1994 M6.7 Northridge earthquake was one such blind fault that produced over $40 billion in damage. This earthquake has been often characterized as occurring on a "previously undiscovered" fault. The fault responsible for the 1994 earthquake was, however, seismically active in the years prior to the earthquake [*Seeber et al.,* 2001] and such south-dipping faults had been previously identified in this area based on subsurface well data [e.g., *Hopps et al.,* 1992; *Yeats et al.,* 1994; *Yeats and Huftile,* 1995]. Because of this recognized need, several agencies, including the Southern California Earthquake Center (SCEC) and the US Geological Survey RELM project, have targeted the identification and mapping in 3D of active faults in southern California as one of their primary scientific objectives.

Recently, several groups have developed improved catalogs of the earthquake activity in southern California (**Fig.1**) [e.g., *Seeber and Armbruster,* 1995; *Hauksson,* 2000; *Richards-Dinger and Shearer,* 2000]. These catalogs comprise over 300,000 earthquake hypocenters since 1988 and over 200,000 well-determined earthquake focal mechanisms. Although many of the earthquakes do occur along mapped surface traces of major faults, many still do not. These extensive earthquake catalogs need to be carefully examined and analyzed—not only for the accuracy and resolution of the earthquake hypocenters [e.g., *Richards-Dinger and Ellsworth,* 2001]—but also for the spatial pattern of fault slip and the orientation of 3D fault surfaces. Rupture along major through-going faults in southern California appears to be strongly affected by local fault geometry and velocity structure, as well as the sense of slip and relative orientation of secondary structures, such as left-lateral conjugate faults, tear faults, and basal detachments [*Nicholson et al.,* 1986; *Nicholson and Lees,* 1992; *Lees and Nicholson,* 1993; *Seeber and Armbruster,* 1995; *Nicholson,* 1996; *Seeber et al.,* 2001]. Identification of these features, especially at seismogenic depths, often depends on careful kinematic analysis of the relocated earthquake hypocenters and focal mechanisms in both space and time.

To address these issues and as a prototype for a more regionally extensive program, a systematic study of the seismicity in one particular area of southern California was conducted to map active subsurface fault planes in 3D, and to help develop a usable, accessible 3D database of these mapped subsurface structures. Active subsurface faults in and around the Santa Barbara–Ventura area along and within the western Transverse Ranges were investigated. This area included major active strands of the North Channel, Pitas Point, Red Mountain, Arroyo Parida, and Santa Ynez faults. The project largely consisted of detailed kinematic analysis of accurate earthquake hypocenters and focal mechanisms to resolve 3D fault planes and patterns of strain accommodation. Where available, other sets of geologic and geophysical data, including surface topography, gravity, geologic mapping, and subsurface well and seismic reflection data were also used. The results were then incorporated into the on-going development of the SCEC digital 3D Community Fault Model (CFM) of subsurface structure for southern California [*Plesch et al.,* 2003] available at: http://structure.harvard.edu/cfm/.

The primary datasets used in the analysis were existing catalogs of relocated earthquake hypocenters and focal mechanisms. **Figure 1** shows a map view of over 310,000 of these

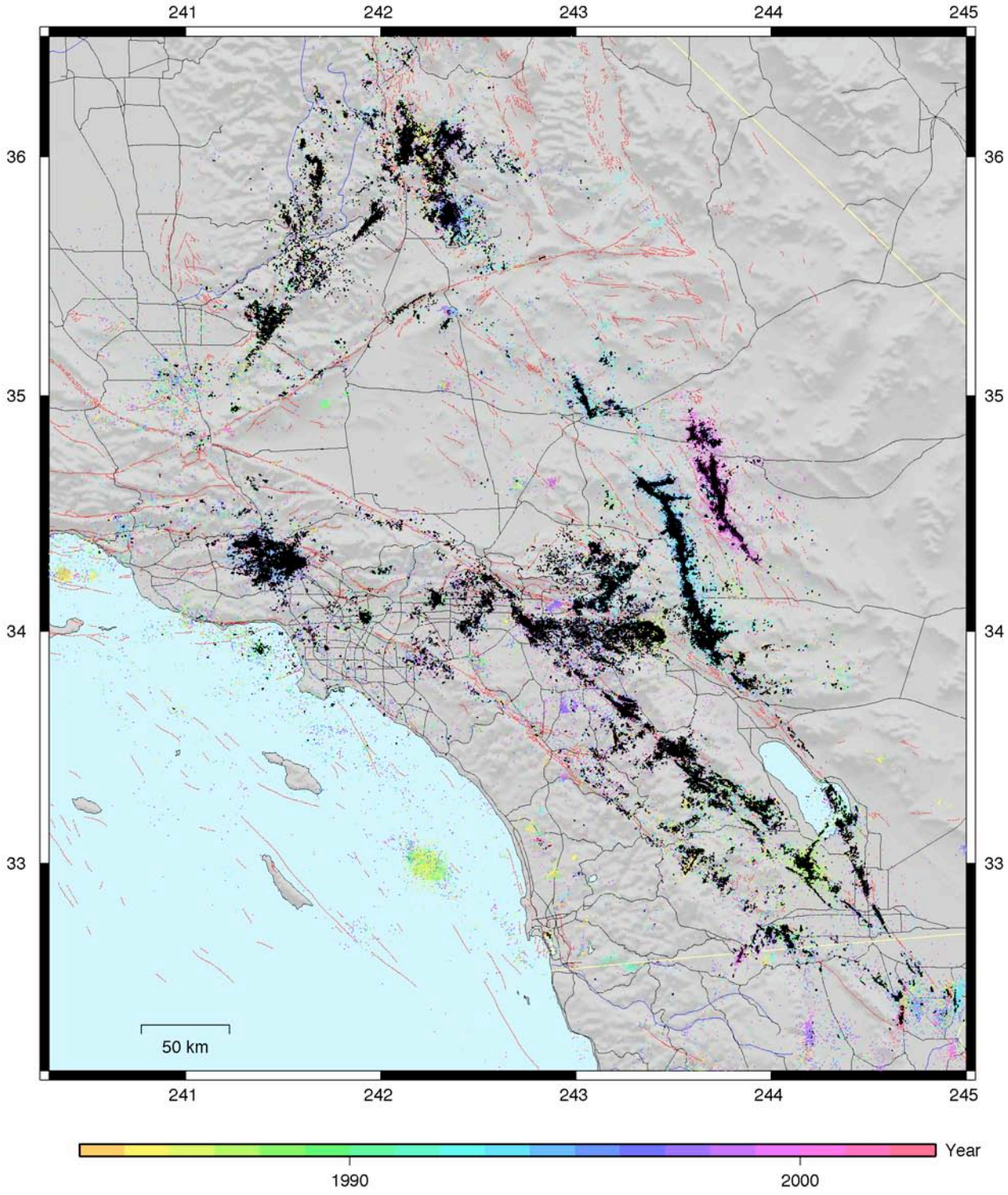

Figure 1. Over 310,000 relocated earthquake epicenters (1988-1999) using a 3D velocity model for southern California [Hauksson, 2000] (black dots) superimposed on top of another set of relocated events based on source specific station terms [Richards-Dinger and Shearer, 2000] color coded by year of occurrence.

relocated hypocenters using a 3D velocity model [*Hauksson,* 2000] as well as a similar set of relocated events based on source specific station terms [*Richards-Dinger and Shearer,* 2000]. These results, in combination with available earthquake focal mechanisms, can be analyzed for spatial alignments of hypocenters and focal mechanism nodal planes in space and time (i.e., 4D).

This kinematic technique of using the spatial and temporal distribution of earthquake hypocenters and focal mechanisms to define the geometry and slip of active subsurface faults has proven to be very effective in southern California [*Nicholson et al.,* 1986; *Nicholson and Seeber,* 1989; *Seeber and Armbruster,* 1995; *Seeber et al.,* 2001]. The power of this technique lies in the internal consistency between two completely independent datasets: (1) the spatial distribution of the earthquake hypocenters in 3D defined by earthquake travel-times, and (2) the kinematic compatibility of the orientation and sense of slip in 3D along individual nodal planes defined by earthquake focal mechanisms. Examination of the earthquake hypocenters alone is not sufficient. This is because questions and uncertainties can arise when well-defined planar features defined by seismicity are inconsistent with the available focal mechanism or first-motion data [*Shearer,* 1998]. In this latter case, other geologic (and possibly non-elastic) processes, such as basin sediment compaction, may be playing an important role in controlling the observed seismic deformation [*Nicholson et al.,* 2000].

This process of using large numbers of microearthquake hypocenters and focal mechanisms to identify and define active subsurface faults is most effective when the seismicity data can be combined with other geologic and geophysical data, and the kinematic analysis can be done in 4 dimensions. At UCSB, we have been working to improve the 3D visualization and analytical tools needed to carefully study such integrated datasets in both space and time [*Nicholson and Lees,* 1994a; *Lees,* 1995; *Green,* 1998]. These computer analysis and visualization tools are both UNIX-based and web-based programs. One such tool is Xmap8. Xmap8 (now called Geotouch) is an interactive UNIX-based computer program for 3D GIS, developed by Jonathan Lees (http://www.unc.edu/~leesj/Geotouch/), in collaboration with people at UCSB [*Nicholson and Lees,* 1994a; *Lees,* 1995]. This program was specifically designed to input large numbers of relocated earthquake hypocenters and focal mechanisms (e.g., **Fig.2**) [*Nicholson and Lees,* 1994b], analyze and visualize these data in 3D (i.e., from all directions including map and cross section), select individual nodal planes that are kinematically compatible with hypocentral alignments, and output the resulting selected events to help define 3D fault surfaces.

Figure 2 shows how this procedure works. On the left are focal mechanisms from the 1992 M6.1 Joshua Tree sequence. Individual fault surfaces are hard to distinguish in this plot. On the right, only single nodal planes of individual focal mechanisms are shown. These nodal planes were chosen as representing individual fault slip surfaces (as opposed to the auxiliary plane) based on the predominant orientation and kinematic alignment of the events in both space and time. This plot shows an unusual and complex fracture network involving predominantly north-south-trending right-lateral faults (involved in the main shock rupture), and ENE-trending left-lateral secondary structures, some of which also exhibit normal slip [*Nicholson and Lees,* 1994]. By carefully identifying and mapping such complex fracture networks, the seismic hazard and behavior of such complex fault systems can then be better defined and understood.

Results

The purpose of this project is to identify and map in 3D active subsurface faults based primarily on the kinematic alignment of earthquake nodal planes and the consistency of slip and the pattern of seismic strain in space and time rather than just the distribution of earthquake

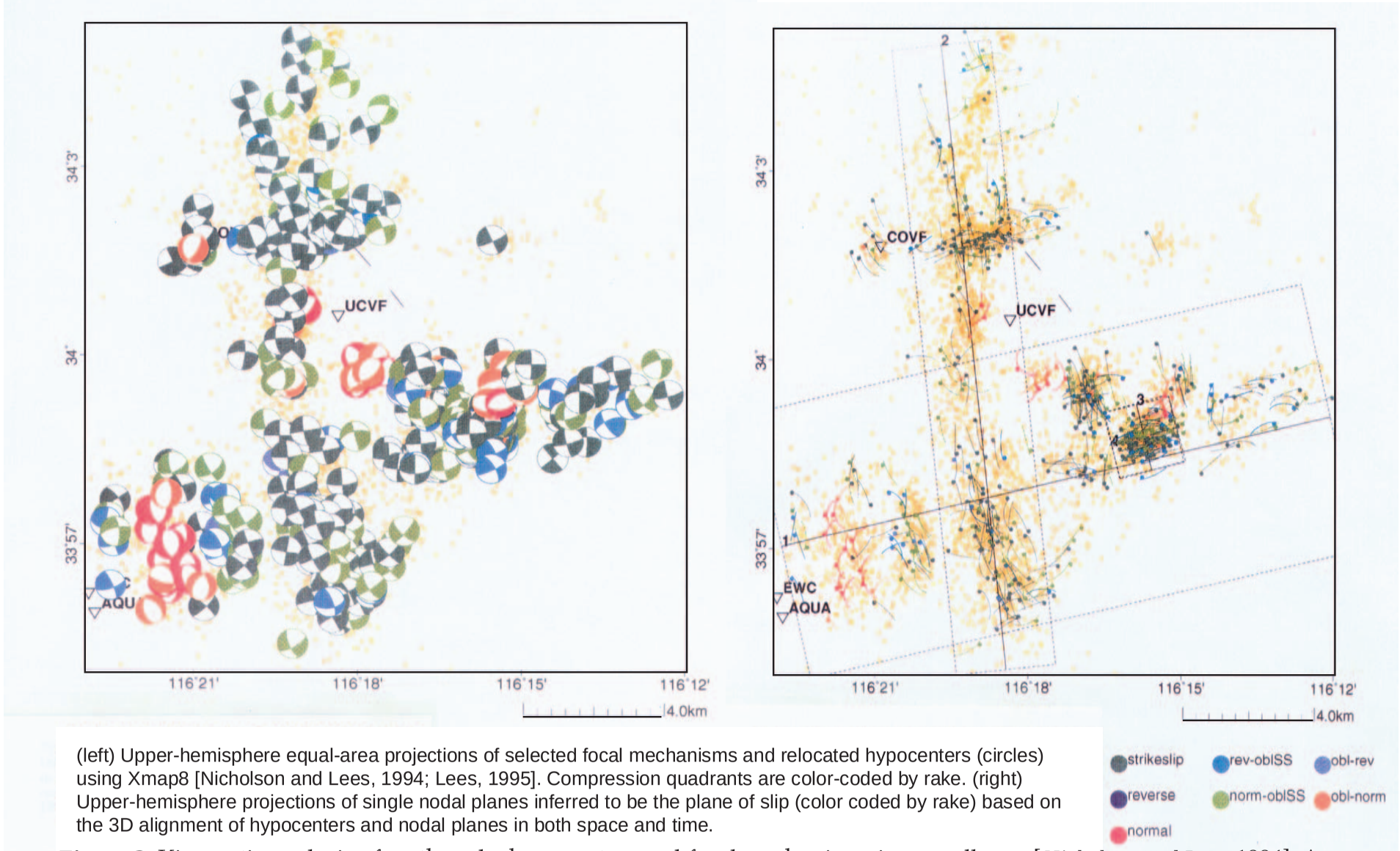

(left) Upper-hemisphere equal-area projections of selected focal mechanisms and relocated hypocenters (circles) using Xmap8 [Nicholson and Lees, 1994; Lees, 1995]. Compression quadrants are color-coded by rake. (right) Upper-hemisphere projections of single nodal planes inferred to be the plane of slip (color coded by rake) based on the 3D alignment of hypocenters and nodal planes in both space and time.

Figure 2. Kinematic analysis of earthquake hypocenters and focal mechanisms in a small area [*Nicholson and Lees*, 1994]. Area shown is the 1992 Joshua Tree earthquake region. (left) For earthquakes with focal mechaism 'beach-ball' plots, the pattern of faulting is difficult to evaluate. (right) When only single slip planes are plotted, pattern of faulting is easier to determine. Pattern exhibits a fracture network of active north-south trending faults and nearly orthogonal ENE-trending secondary structures.

hypocenters. Only relocated earthquakes were used (e.g, **Fig.1**). This is particularly important in dealing with earthquakes in Southern California owing to the large observed variations in crustal seismic velocities. To demonstrate the value and validity of this technique, **Figure 3** shows a map and vertical cross section of the 1986 M6 North Palm Springs earthquake sequence located along the Banning strand of the San Andreas fault in the northern Coachella Valley [*Nicholson,* 1996]. The hypocenters were part of a detailed, joint relocation and 3D tomographic velocity inversion [*Nicholson and Lees,* 1992]. Kinematic analysis of the relocated hypocenters and focal mechanisms show a consistent pattern of right-lateral to right-oblique reverse slip on the main shock fault plane that dips northeast at 45° to 50°. Secondary structures, including the near-vertical, left-lateral Morongo Valley fault (MVF) and a low-angle detachment surface were also active as part of this sequence and identified by the kinematic analysis (**Fig.3**).

These secondary structures, although releasing little seismic moment themselves are, nonetheless, critically important. Such high-angle cross faults and low-angle detachments appear to strongly control dynamic slip during main shock ruptures [e.g., *Nicholson et al.,* 1986; *Hudnut et al.,* 1989; *Nicholson and Seeber,* 1989; *Nicholson,* 1996; *Seeber et al.,* 2001] and provide a mechanism for mechanically layering the seismogenic crust [*Webb and Kanamori,* 1985, *Nicholson et al.,*1986; *Fuis et al.,* 2001]. The pattern of strain accommodation (and focal mechanisms) may thus change above and below such mid-crustal detachment surfaces. In fact, microearthquakes above and below a depth of about 12 km in San Gorgonio Pass do seem to exhibit such a change in spatial distribution and focal mechanism behavior, consistent with the depth of the detachment identified in **Figure 3** [*Nicholson et al.,* 1986; *Nicholson,* 1996].

Active Faults Beneath the Western Transverse Ranges

For earthquakes in the Santa Barbara–Ventura study area, kinematic analysis of hypocenters and focal mechanisms also shows a consistent pattern of surface and subsurface deformation (**Fig.4**). Relocated earthquake hypocenters and revised focal mechanisms—derived from an improved velocity model that accounts for the low-velocity sediments in the Ventura basin—were used to define a set of low-to-moderately north-dipping structures, including the Pitas Point (PPF) and Red Mountain faults (RMF). Focal mechanisms were consistent with reverse to slightly oblique reverse slip on these surfaces. In addition, two steeply south-dipping structures with the geometry of 'back-thrusts' were identified that would coincide with the Arroyo Parida (APF) and Santa Ynez faults (SYF). These latter, typically more steeply dipping structures currently exhibit predominantly left-lateral slip as shown by more recent geologic fault offsets and focal mechanism solutions [*Dibblee,* 1986, 2002; *O'Connell,* 1995; *Nicholson and Kamerling,* 1998; *Keller and Gurrola,* 2000]. More recent well-located earthquake hypocenters and focal mechanisms continue to define this same subsurface pattern of fault geometry and slip.

All these faults defined at depth by planar zones of seismicity coincided with mapped traces of the faults based either on surface geology [*e.g., Dibblee,* 2002], subsurface well data [*e.g., Hopps et al.,* 1992; *Redin et al.,* 1998] or near-surface imaging in industry multichannel seismic (MCS) reflection data. **Figure 5** shows an example of these MCS data collected just offshore across the Red Mountain fault. The data clearly show offset and deformed strata consistent with the south and north strands of the Red Mountain fault. The data also show folding of footwall sediments, indicating the presence of additional active south-verging thrust faults propagating farther south out into the basin, such as the Pitas Point fault (PPF) shown in **Figure 4**.

What is most interesting, in addition to the four major known faults discussed above, was the discovery of yet another active structure in the footwall of the Santa Ynez fault. In 1996, a

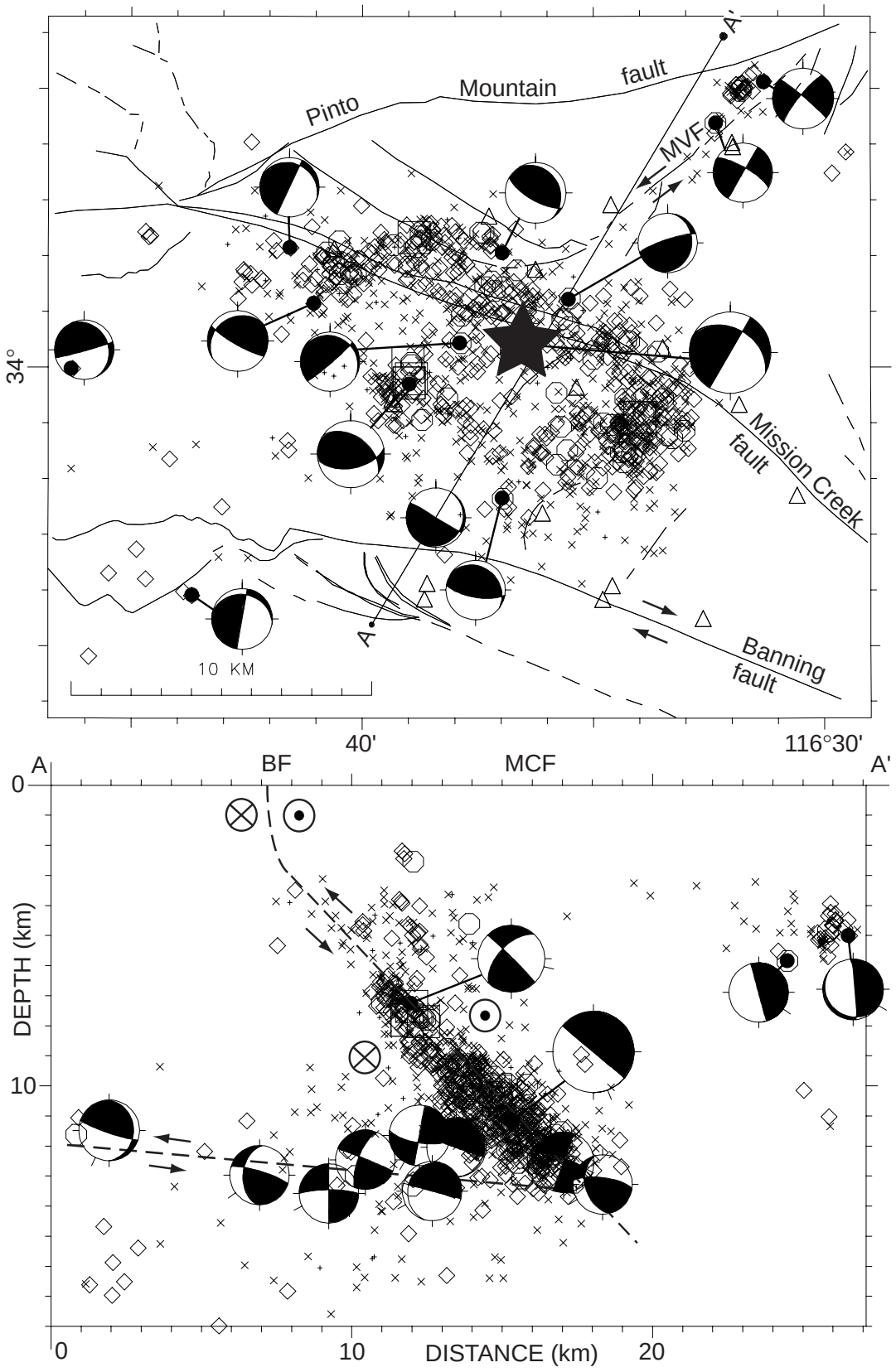

Figure 3. Map and cross section of the 1986 M6 North Palm Springs sequence showing the activation of both high-angle and low-angle structures to accommodate oblique slip.

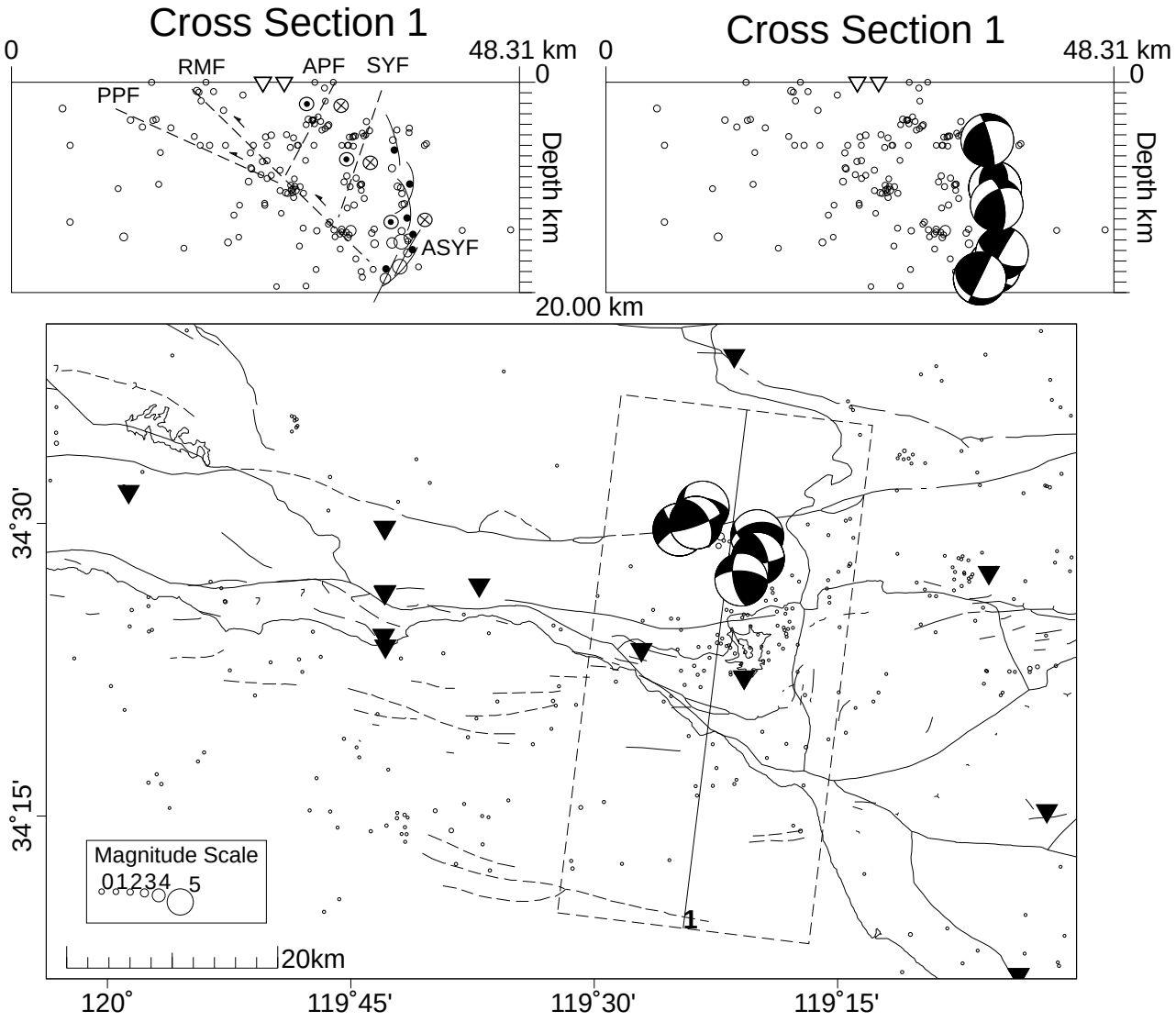

Figure 4. Map and vertical cross sections of relocated seismicity (1994-1996) and the 1996 M4.6 Ojai sequence. Upper- (map) and front- (cross section) hemisphere projection focal mechanisms of the Ojai events and interpretations of active subsurface faults are shown. Earthquakes define three major faults in the hanging-wall of the Red Mountain fault (RMF): Arroyo Parida fault (APF); Santa Ynez fault (SYF); and a curviplanar fault whose surface trace projection would also correspond with the SYF. We call this the Ancestral Santa Ynez fault (ASYF). In the footwall of the RMF, seismicity also appears to define a south-verging Pitas Point fault (PPF) beneath Ventura Avenue Anticline that intersects and merges with the RMF at a depth of about 9–10 km. This basic fault geometry is observed farther west, based on well, seismicity and seismic reflection data.

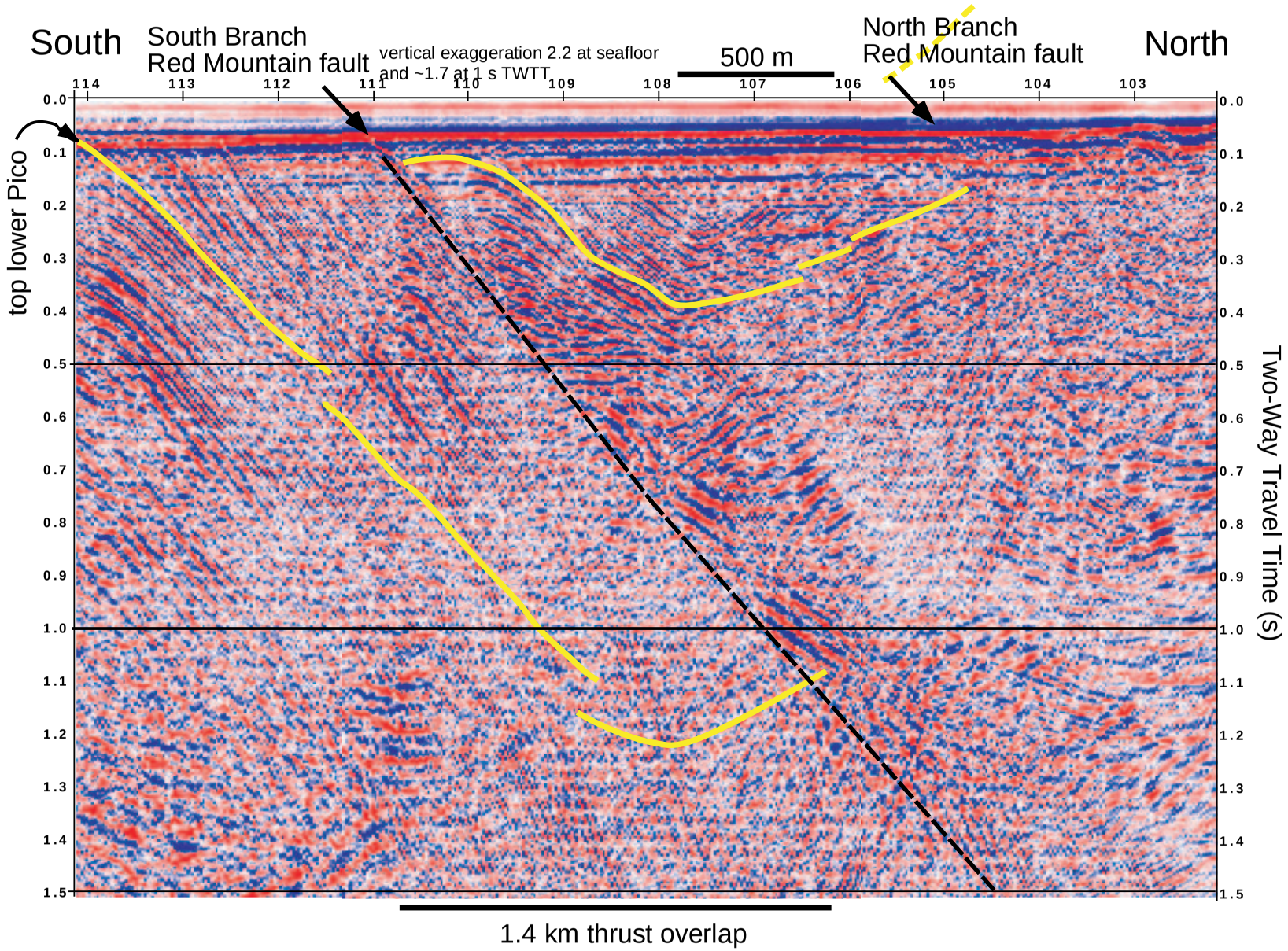

Figure 5. Migrated industry seismic line across south branch of Red Mountain fault (arrow) showing offset stratigraphy. Note tight folding in footwall of south branch RMF requiring presence of additional active faults. Interpreted horizon (yellow) is top lower Pico Formation (~1.8 Ma). Such data provided added constraints on active fault geometry.

particular earthquake sequence occurred near Ojai, whose M4.6 main shock and aftershocks defined a previously unsuspected non-planar fault extending to a depth of about 18 km (**Fig.4**). The extrapolated surface trace of this fault would also coincide with the location of the Santa Ynez fault. We call this deformed active feature the Ancestral Santa Ynez fault (ASYF). The fault geometry defined by the earthquake hypocenters match the changing dip with depth of the nodal planes in the individual focal mechanism solutions, enabling the complicated, curved 3D geometry of this blind oblique-reverse fault to be determined with a high degree of confidence. The existence of this previously unsuspected fault may explain why the dip of the Santa Ynez fault at the surface is often mapped as south-dipping to the west and north-dipping to the east [e.g., *Dibblee,* 1988; *Hopps et al.,* 1992]. The western surface segment may be the traditional Santa Ynez fault, while the trace mapped farther east may actually correspond to the Ancestral Santa Ynez fault, which should be north-dipping at shallow depth as shown in **Figure 4**.

The important implications of these kinematic results based on seismicity are three fold:

(1) Deformation in the footwall of the Red Mountain fault, including the Ventura Avenue Anticline, is predominantly associated with south-verging thrust faults, like the Pitas Point fault;

(2) All these structures, including the Pitas Point fault, Red Mountain fault, Arroyo Parida fault (and its segments farther west—the Mission Ridge and Moore Ranch faults), as well as other segments identified offshore like the North Channel, Rincon, Coal Oil Point and Lavigia faults, all merge at depth to form a single active North Channel–Pitas Point–Red Mountain fault system;

(3) This fault system accommodates left oblique reverse motion by strain partitioning of dip-slip components onto predominantly low-to-moderate-angle north-dipping thrust faults (PPF, RMF) and strike-slip components onto high-angle predominantly south-dipping left-slip faults (APF).

Integration of Subsurface Seismicity, Seismic Reflection and Well Data

Besides seismicity data, other geological and geophysical data can be used to help identify and map in 3D various fault surfaces, including well and seismic reflection data, and previously published structure maps and cross sections. These data can provide important independent control on 3D fault geometry and other geologic reference surfaces [e.g., *Wright,* 1991; *Hopps et al.,* 1992; *Yeats et al.,* 1994; *Tsutsumi and Yeats,* 1999; *Shaw and Shearer,* 1999]. This includes using marine multichannel seismic reflection (MCS) data to map low- and high-angle faults offshore southern California [*Nicholson et al.,* 1996; 2004], and using seismic reflection and well data to produce 3D structure contour maps of various stratigraphic (time) horizons and shallow 3D fault surfaces in the Santa Barbara Channel [*Kamerling et al.,* 2003]. The MCS data shown in **Figure 5** provide information on both the location and geometry of the Red Mountain fault, as well as the geometry of deformed stratigraphic reference horizons, such as the top Lower Pico surface dated at about 1.8 Ma (yellow line) [*Kamerling et al.,* 2001, 2003]. By using extensive grids of such MCS data, and correlating the reflections with stratigraphy identified in coreholes and wells, these stratigraphic reference horizons and fault surfaces can be mapped in 3D.

Figure 6 shows an oblique 3D view of some of the resulting mapped 3D surfaces for the Santa Barbara area, together with surface topography and relocated earthquake hypocenters from the 1978 M5.9 Santa Barbara earthquake [*Kamerling et al.,* 2003]. The strong correlation between the earthquakes at depth and the fault surfaces and folding imaged by the MCS data demonstrates the validity and capability of these integrated data sets to define the geometry of active 3D fault surfaces to seismogenic depths.

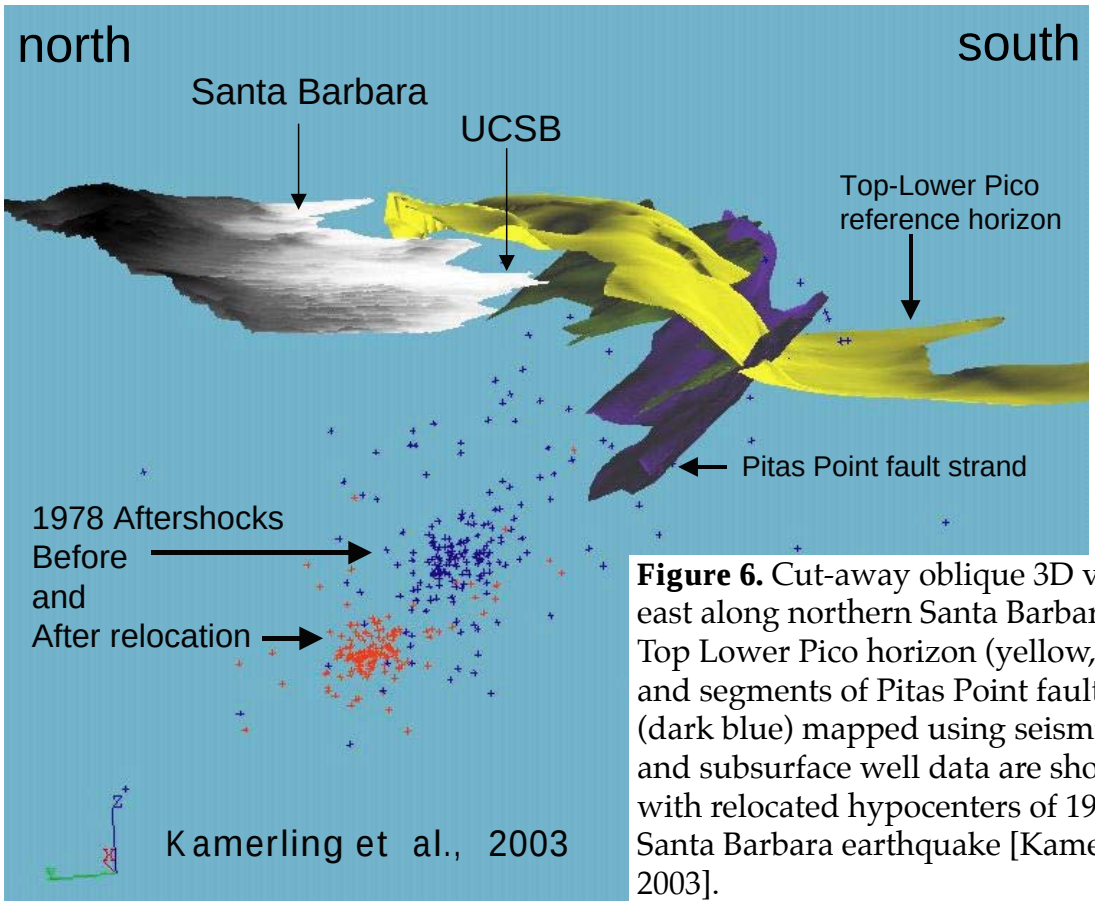

Figure 6. Cut-away oblique 3D view looking east along northern Santa Barbara Channel. Top Lower Pico horizon (yellow, ~1.8 Ma) and segments of Pitas Point fault strand (dark blue) mapped using seismic reflection and subsurface well data are shown along with relocated hypocenters of 1978 M5.9 Santa Barbara earthquake [Kamerling et al., 2003].

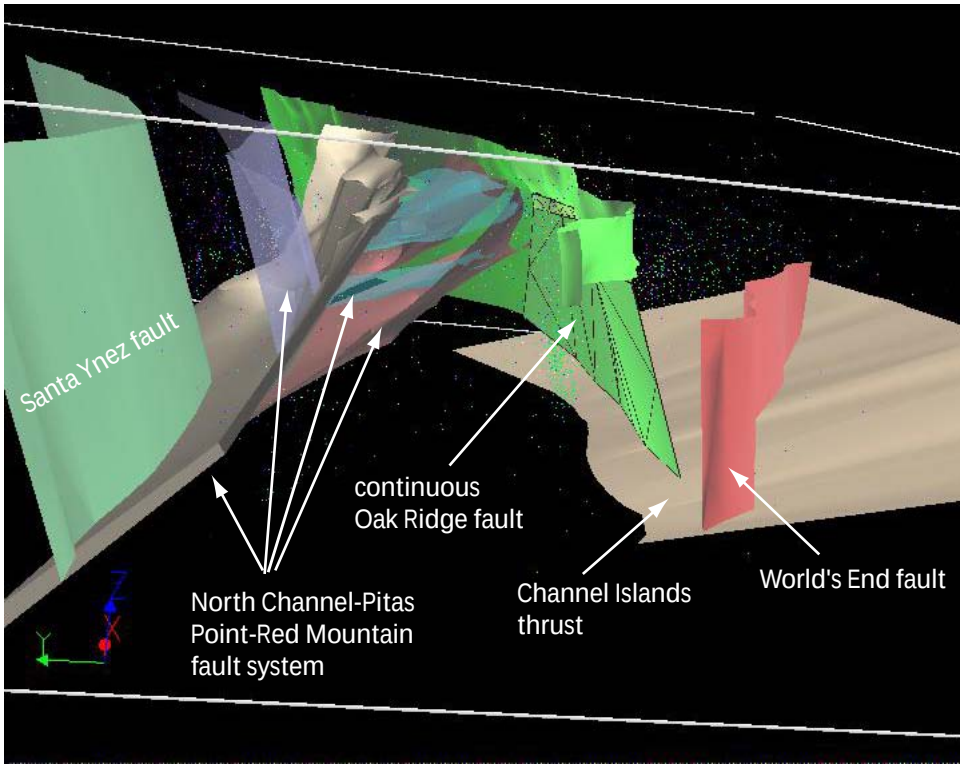

Figure 7. Oblique 3D view looking east of our alternate representation within SCEC Community Fault Model (CFM) of active North Channel-Pitas Point-Red Mountain fault system that is internally consistent and kinematically compatible. North Channel, Pitas Point, Red Mountain and Arroyo-Parida fault segments now all merge at depth to form a single active fault system [Kamerling et al., 2003].

More importantly, the 3D fault surfaces, deformed stratigraphic reference horizons and other digital datasets can be input into 3D visualization and analysis programs, like gOcad and UNFOLD for more detailed quantitative evaluation. For example, these programs allow the quantitative restoration of deformed stratigraphic horizons in 3D to invert for finite strain fields, fault slip, and subsurface fault geometry [*Gratier et al.,* 1991, 1999; *Thibaut et al.,* 1996; *Kamerling et al.,* 1998; *Sorlien et al.,* 2000]. 3D map restoration of the folded and faulted top Lower Pico horizon (yellow, **Figs.5&6**) indicates that the cumulative vertical strain across the Pitas Point and North Channel fault strands since deposition amounts to nearly 3 km, with at least an equal amount of vertical slip accommodated by various strands of the Red Mountain fault [*Kamerling et al.,* 2003]. This suggests that much of the measured geodetic strain rate using GPS of about 6 mm/yr across this area [e.g., *Larsen et al.,* 1993] may be localized at depth on the master fault of the North Channel–Pitas Point–Red Mountain fault system.

Development of a Combined, Integrated 3D Community Fault Model

Accurate description of the 3D geometry of active faults at depth is thus crucial to understanding their behavior, evolution and seismic hazard. Several fault databases often include only a digital map surface trace, and various strikes and dips at different points. To infer fault geometry at depth, this requires one presumes that faults are planar and continue at depth with constant dip. The geometry of the Ancestral Santa Ynez fault (ASYF) in **Figure 4** shows that this is often not the case. Another example, based on seismicity, focal mechanisms, gravity, and surface mapping, is the southern San Andreas fault, which defines a complicated 3D geometry as it exits the northern Coachella Valley and traverses San Gorgonio Pass [*Nicholson,* 1996; *Yule and Sieh,* 2001]. The San Cayetano, Oak Ridge, Santa Susana, Red Mountain, Cucamonga, and several other major active faults within the Transverse Ranges also exhibit significant non-planar geometry [*Yeats,* 1981; *Wright,* 1991; *Hopps et al.,* 1992; *Yeats et al.,* 1994; *Kamerling et al.,* 2001; *Nicholson et al.,* 2001]. This 3D geometry can significantly affect dynamic earthquake ruptures, and thus the resulting estimates of inferred ground motion and seismic hazard.

In addition to accurate fault geometry, the resulting set of 3D fault surfaces must be internally consistent and kinematically compatible. Major faults that exhibit contemporaneous fault offset or displacement can not mutually cross cut each other, or they quickly become incompatible to accommodate further finite strain. **Figure 7** shows an oblique 3D view looking east of alternative representations of digital 3D fault surfaces provided by us to the SCEC 3D Community Fault Model (CFM), together with relocated earthquake hypocenters [*Hauksson,* 2000], of the Santa Barbara–Ventura area. These are the faults which we feel provide a mutually compatible fault set to accommodate regional crustal strain. Important characteristics to note are: (1) a single, master south-verging North Channel–Pitas Point–Red Mountain fault system (red, blue, grey surfaces), which includes more steeply dipping fault strands, such as the Arroyo Parida–Mission Ridge–Moore Range faults (purple surface), in its hanging wall; and (2) a steeply south-dipping, non-planar Oak Ridge fault system that is continuous at depth between its onshore and offshore segments. Left-lateral oblique reverse motion accommodated by the North Channel–Pitas Point–Red Mountain fault system is thus partitioned into predominantly strike-slip motion on the steeply dipping hangingwall strands, such as the Arroyo Parida fault (**Fig.4**), while vertical motions are accommodated by predominantly dip-slip motion on the low-to-moderately north-dipping Red Mountain, North Channel and Pitas Point fault strands.

Conclusions

Rupture along major through-going faults in southern California, such as the 1986 North Palm Springs earthquake along the San Andreas fault (**Fig.3**) appears to be strongly affected by local fault geometry, as well as the sense of slip and relative orientation of secondary structures, such as left-lateral conjugate cross faults, tear faults, and low-angle basal detachments. Identification of these features, especially at seismogenic depths, often depends on careful kinematic analysis of the earthquake hypocenters and focal mechanisms in both space and time.

Careful evaluation of the seismicity patterns in and around the Santa Barbara-Ventura area of the western Transverse Ranges were used to identify and map active subsurface fault surfaces in 3D, and to improve our understanding of the regional tectonic framework controlling contemporary crustal deformation. This area includes various strands of the North Channel, Pitas Point, Red Mountain, Arroyo Parida, and Santa Ynez faults. Detailed kinematic analysis of accurate relocated earthquake hypocenters and focal mechanisms were used to resolve 3D fault planes and patterns of strain accommodation. Where available, other sets of geologic and geophysical data, including topography, gravity, geologic mapping, seismic reflection and subsurface well data were also used. The results suggest that several of these major active fault strands, both onshore and offshore of southern California, merge at depth to form a single North Channel–Pitas Point–Red Mountain fault system. In addition, the 3D geometry and slip on these active subsurface faults is consistent with the partitioning of oblique crustal strain on sets of high- and low-angle structures to accommodate oblique contemporary plate motion.

Data Availability

Digital representations of 3D fault surfaces for the Santa Barbara–Ventura area are available from the SCEC 3D Community Fault Model website (http://structure.harvard.edu/cfm/). Additional structure contour maps of specific stratigraphic reference horizons (Near-Top Pico, Top Lower Pico, etc.) are available from http://www.crustal.ucsb.edu/projects/vbmrp.

Reports published

Kamerling, M.J., C.C. Sorlien, and C. Nicholson, 3D development of an active oblique fault system, northern Santa Barbara Channel, California, *Seismological Research Letters*, **v. 74**, n. 2, p. 248, 2003.

Nicholson, C., C.C. Sorlien and J.R Childs, Southern California Imaging Project (SCIP): Archiving and using industry data to evaluate plate boundary deformation, *Seismological Research Letters,* **v.75**, n.2, p.258, 2004.

Nicholson, C., C.C. Sorlien and J.R Childs, GENII: A developing consortium to archive and use industry data to evaluate plate boundary structure, deformation and evolution, *16th Annual IRIS Workshop*, Tucson, AZ, 2004.

Non-technical Summary

Kinematic analysis of earthquake locations and directions of fault slip are used to define the geometry of active subsurface faults in 3 dimensions and to better understand the regional pattern of contemporary crustal strain. Earthquakes in the northern Coachella Valley reveal a complex pattern of oblique-reverse slip on a moderately dipping Banning strand of the San Andreas fault, interacting with secondary structures, including a high-angle left-slip cross fault and a low-angle detachment to control fault slip. In the Santa Barbara–Ventura area, earthquake patterns reveal

several major fault strands merging at depth to form a single south-verging North Channel–Pitas Point–Red Mountain fault system. This fault system accommodates oblique crustal strain through partitioning of horizontal motions on predominantly strike-slip steeply south-dipping faults (such as the Arroyo Parida fault strand) and vertical motions on predominantly low-to-moderately north-dipping thrust faults, like the Red Mountain and Pitas Point fault strands.

Bibliography

Dibblee, T.W, Jr., Geologic map of the Santa Barbara quadrangle, Ehrenspeck, ed., *Dibblee Geolgical Foundation Map DF06*, Santa Barbara, CA, 1986.

Dibblee, T.W., Jr. Geology of the Ventura Basin area, in *Ventura Basin: Geologic Introduction and Field Trip Guidebook,* M.H.Link, ed., *Pacific Section–Am. Assoc. Petrol. Geologists Publ.,* p. 7-18, 1988.

Dibblee, T.W., Jr., Geology of the Santa Ynez Mountains, *Dibblee Geological Foundation Georeferenced Digital Quadrangles,* Santa Barbara, CA, 2002.

Fuis, G.S., Ryberg, T., Godfrey, N.J., Okaya, D.A., and Murphy, J.M., 2001, Crustal structure and tectonics from the Los Angeles basin to the Mojave Desert, southern California, *Geology*, **29**, p. 15-18.

Gratier, J.P., B. Guillier, A. Delorme and F. Odonne, Restoration and balance of a folded and faulted surface by best-fitting finite elements: principles and application, *J. Struct. Geol.,***13,** p. 111-115, 1991.

Gratier, J.-P., Hopps, T., Sorlien, C. C., and Wright, T., 1999, Recent crustal deformation in southern California deduced from the restoration of folded and faulted strata, *Journal of Geophysical Research*, **v. 104**, p. 4887-4899.

Green, L. Development of an interface for 3D visualization of SCEC earthquake data on the World Wide Web, UCSB-SCEC Summer intern, 1998 SCEC Annual Meeting, p.36.

Hauksson, E., Crustal structure and seismicity distribution adjacent to the Pacific and North American plate boundary in southern California, *J. Geophys. Res.,* v.105, n.B6, p. 13,875-13,899 (2000).

Hopps, T.E., H.E. Stark, and R.J. Hindle, Subsurface geology of Ventura Basin, California, *Ventura Basin Study Group Report,* 45 pp., 17 structure contour maps and 84 structure panels comprising 21 cross sections, Rancho Energy Consultants, Inc., Santa Paula, CA, 1992.

Hudnut, K., L. Seeber and J. Pacheco, Cross-fault triggering in the November 1987 Superstition Hills earthquake sequence, southern California, *Geophys. Res. Lett.*, **16**, p. 199–202, 1989.

Kamerling, M.J., C.C. Sorlien, and C. Nicholson (1998), Subsurface faulting and folding onshore and offshore of Ventura basin: 3D map restoration across the Oak Ridge fault, *SCEC 1998 Annual Meeting Report,* Palm Springs, p.68-69.

Kamerling, M.J., C.C. Sorlien, R. Archuleta, and C. Nicholson, Three-dimensional geometry and interactions of faults and structures along the northern margin of the Santa Barbara Channel, California, *Geol. Soc. Am. Abstracts w/Prog.*, **v. 33**, n. 3, p. A41, 2001.

Kamerling, M.J., C.C. Sorlien, and C. Nicholson, 3D development of an active oblique fault system, northern Santa Barbara Channel, California, *Seismol. Res. Lett.*, **v. 74**, p. 248, 2003.

Keller, E.A. and L.D. Gurrola, Earthquake hazard of the Santa Barbara fold Belt, California, *U.S. Geol. Surv. Final Technical Report NEHRP Award 99HQGR0081*, 105 pp., 2000.

Larsen, S.C., D.C. Agnew and B.H. Hager, Strain accumulation in the Santa Barbara Channel: 1970–1988, *J. Geophys. Res.,* **v.98**, p. 2119–2133, 1993.

Lees, J.M., Xmap8: A free computer program for three-dimensional GIS, *Seismol. Res. Lett.,* **v. 66,** p. 33–37 (1995).

Lees, J. M. and C. Nicholson, Three-dimensional tomography of the 1992 Southern California sequence: Constraints on dynamic earthquake rupture?, *Geology,* **21,** p. 387–390 (1993).

Nicholson, C., Seismic behavior of the San Andreas fault in the Northern Coachella Valley, California: Comparison of the 1948 and 1986 earthquake sequences, *Bulletin of the Seismological Society of America,* **86,** n. 5, p. 1331–1349 (1996).

Nicholson, C. and M.J. Kamerling (1998), Reliability of 2D kinematic fold models to infer deep fault structure in the western Transverse Ranges, California, *Proceedings of the NEHRP Conference and Workshop on the Northridge, California Earthquake,* **v. II,** p. 299–306.

Nicholson, C., M.J. Kamerling, and J.N. Brune (2001), Thrust nappes and mega-slides: Implications for active fault geometry, dynamic rupture, and seismic hazard in southern California, Seismol. Res. Lett., **v. 72**, n.2, p. 291.

Nicholson, C. and J.M. Lees, Travel-time tomography in the northern Coachella Valley using aftershocks of the 1986 M_L 5.9 North Palm Springs earthquake, *Geophysical Research Letters,* **19,** p. 1–4 plus cover (1992).

Nicholson, C. and J.M. Lees, Xmap8 — Interactive Color Graphics for Analysis of GIS and 3-D Geophysical Data, Part I: Demonstration and Program Capabilities (abstract), *Eos - Trans. AGU,* **v.75,** p. 456 (1994a).

Nicholson, C. and J. Lees, 3-D analysis of seismicity, focal mechanisms and stress using the 1992 Landers-Big Bear-Joshua Tree earthquake sequences, southern California, *SCEC Annual Report,* **v.2,** F28–F32 (1994b).

Nicholson, C. and L. Seeber, Evidence for contemporary block rotation in strike-slip environments: Examples from the San Andreas fault system, southern California, in *Paleomagnetic Rotations and Continental Deformation,* C. Kissel and C. Laj, eds., Kluwer Academic Publishers, Dordrecht, The Netherlands, 247-280 (1989).

Nicholson, C., L. Seeber, P. Williams and L.R. Sykes. Seismicity and fault kinematics through the eastern Transverse Ranges, California: Block rotations, strike-slip faulting and low-angle thrusts, *Journal of Geophysical Research,* **91,** 4891-4908, (1986a).

Nicholson, C., L. Seeber, P. Williams and L.R. Sykes. Seismic evidence for conjugate slip and block rotation within the San Andreas fault system, southern California, *Tectonics,* **5,** 629-648 (1986b).

Nicholson, C., C.C. Sorlien and J.R Childs, Southern California Imaging Project (SCIP): Archiving and using industry data to evaluate plate boundary deformation, *Seismol. Res. Lett.,* **v.75**, n.2, p.258, 2004.

Nicholson, C., C.C. Sorlien, M.J. Kamerling, J.-P. Gratier, and L. Seeber (2000), Influence of active subsidence, compaction, and footwall defomation on estimates of fault slip, geodetic strain, and seismic hazard*, Eos (Trans. AGU),* **v. 81**, n.48, p. F1213.

Nicholson, C., C.C. Sorlien, and M.R. Legg, Crustal Imaging along the California Continental Borderland: Miocene extension, rotation, and tectonic inversion related to an evolving transform system, *7th International Symposium on Deep Seismic Profiling,* Asliomar, California, Sept. 15–20, 1996.

O'Connell, D., Earthquake locations, focal mechanisms, and GPS near Ventura, Western Transverse Ranges, California: The crust has a thick skin, *Eos (Trans. AGU),* **76,** n.46, p. F141 (1995).

Plesch, A., J.H. Shaw, and SCEC CFM Working Group, SCEC CFM – A WWW accessible Community Fault Model for Southern California, *Eos (Trans. AGU)*, **v.84**, n.46, Abstract S12B-0395 (2003).

Richards-Dinger, K.B. and W.L. Ellsworth, A comparison of earthquake (Re)Location methods *Seismol. Res. Lett,* **v.72**, n.2, p. 229 (2001).

Richards-Dinger, K.B. and P.M. Shearer, Earthquake locations in southern California obtained using source specific station terms, *J. Geophys. Res.,* **v.105**, n.B5, p. 10,939-10,960 (2000).

Seeber, L. and J.G. Armbruster, The San Andreas fault system through the Transverse Ranges as illuminated by earthquakes, *J. Geophys. Res.,* **v. 100,** p.8285–8310, 1995.

Seeber, L., J.G. Armbruster, and P. Geiser, The 1994 Northridge and 1971 fault ruptures and surrounding seismogenic faults as illuminated by small earthquakes, *Geol. Soc. Am. Abstracts w/Prog.*, **v. 33**, n.3, p.A-63 (2001).

Shaw, J.H. and P.M. Shearer, An elusive blind-thrust fault beneath metropolitan Los Angeles, *Science,* **v.283**, p. 1,516-1,518, 1999.

Shearer, P.M., Evidence from a cluster of small earthquakes for a fualt at 18 km depth beneath Oak Ridge, soutehrn California, *Bull. Seism. Soc. Am.,* **v.88**, p. 1327-1336, 1998.

Sorlien, C.C., J-P Gratier, B.P. Luyendyk, J.S. Hornafius, and T.E. Hopps, Map restoration of folded and faulted late Cenozoic strata across the Oak Ridge fault, onshore and offshore Ventura basin, California, *Geol. Soc. Am. Bull.,* **v.112,** n.7, p. 1080-1090 (2000).

Thibaut, M., J.P. Gratier, M. Léger, and J.M. Morvan (1996). An inverse method for determining three-dimensional fault geometry with thread criterion: application to strike-slip and thrust faults, *J. Structural Geol.,* **v.18,** p. 1127–1138.

Tsutumi, H. and R.S. Yeats, Tectonic setting of the 1971 and 1994 Northridge earthquakes in the San Fernando Valley, California, Bull. Seismol. Soc. Am., v.89, n.5, p. 1,232-1,249 (1999).

Webb, T. H. and H. Kanamori, Earthquake focal mechanisms in the Eastern Transverse Ranges and San Emigdo Mountains, southern California, and evidence for a regional decollement, *Bull Seism. Soc. Am.,* **75,** p. 737-757, 1985.

Wright, T.L., 1991, Structural geology and tectonic evolution of the Los Angeles basin, California, in *Active Tectonic Basins,* T.K. Biddle, ed., *AAPG Memoir 52*, p.35-134.

Yeats, R.S. and G.J. Huftile (1995). Oak Ridge fault system and the 1994 Northridge, California, earthquake, *Nature,* **v.373,** p. 418–420.

Yeats, R.S., Deformation of a 1 Ma datum, Ventura basin, *U.S. Geol. Surv. Final Rep.,* 27 pp., 1981.

Yeats, R.S., G.J. Huftile, and L.T. Sitt, Late Cenozoic tectonics of the east Ventura basin, California, Am. Asoc. Petrol. Geol. Bull., v. 78, p.1040-1074, 1994.

Yule, D. and K. Sieh, The paleoseismic record at Burro Flats: Evidence for a 300-year average recurrence for large earthquakes on the San Andreas fault in San Gorgonio Pass, southern California, *Geol. Soc. Am. Abstracts w/Prog.*, **v. 33**, n.3, p.A-31 (2001).